Eur. Phys. J. D **7**, 467–473 (1999)

THE EUROPEAN PHYSICAL JOURNAL D

EDP Sciences

Saturation of the weak probe amplification in a strongly driven cold and dense atomic cloud

L. Khaykovich[a], N. Friedman, and N. Davidson

Department of Physics of Complex Systems, Weizmann Institute of Science, Rehovot 76100, Israel

Received 3 November 1998 and Received in final form 5 March 1999

Abstract. We present an experimental and theoretical investigation of the weak probe amplification in a cold and optically thick atomic cloud that is highly driven by a strong pump laser. We find that for high optical densities the probe amplification is strongly saturated. We compare our saturation measurements with a model based on dressed-atom population equalization due to re-scattering of spontaneous emission. Good agreement between theory and experiment is obtained only when corrections due to multiple scattering are included.

PACS. 32.80.Pj Optical cooling of atoms, trapping – 32.80.-t Photon interactions with atoms – 32.50.+d Fluorescence, phosphorescence (including quenching)

1 Introduction

When an atom is illuminated by a high intensity light field, both its spontaneous emission and absorption spectra are changed. For a two-level atom, the well-known theory developed by Mollow [1,2], describes both changes: the Mollow triplet in the fluorescence spectrum, and the change in the absorption spectrum, including the introduction of amplification in a specific frequency range. This theory was checked experimentally on dilute atomic beams [3] and cold atomic clouds [4,5], and was found to be in good agreement with experimental results. However, when the optical density of the atomic gas in all directions becomes larger than one, the intensity of the spontaneous emission approaches the saturation intensity of the atomic transition. As a result, photon re-scattering becomes significant, and has to be included as a correction for the single atom treatment.

Photon re-scattering and resulting effects such as radiation trapping in cold atomic clouds aroused much interest in recent years [6–9] from both fundamental and practical aspects. Fundamentally, dense and cold atomic clouds enable investigations of various models that describe radiation trapping, such as the Holstein and Payne models [10,11], under conditions where the atom-light interaction is well known and understood, and complications such as Doppler and collisional broadening are strongly suppressed [8]. Cold and dense atomic cloud may serve also as a new environment for the investigation of nonlinear radiation trapping effects [12]. Practically, re-scattering of photons often limits both the density [6] and temperature [7] of laser cooled and trapped atoms. In particular it is the main obstacle for achieving Bose-Einstein condensation using all-optical means [9].

In this work, we investigated Mollow amplification in a cold and optically dense cloud of rubidium atoms under conditions where they essentially behave as two-level atoms. We measured the amplification of a weak probe beam in the presence of a strong pump laser, as a function of the optical density (OD) of the atomic cloud. We found that the amplification is strongly saturated, and does not increase linearly with the OD as expected from the simple theory [2]. We attribute the saturation to re-scattering of spontaneous emission inside the atomic cloud. Since the sidebands of the spontaneous emission spectrum nearly coincide with the frequencies for absorption and amplification in the presence of a strong pump [13], the re-scattering cross-section is large. Therefore, these spontaneous photons compete with the probe beam photons and decrease the possible amplification.

For quantitative description of this novel result, we developed a simple model that is based on the dressed atom picture [13]. In this model, we evaluate the decrease in the population difference between the dressed states, which is caused by re-absorption of spontaneous emission, and the corresponding decrease in the weak probe amplification. We found good agreement between the model and the measured amplification and its saturation for large detuning of the pump laser, where amplification due to nonsecular terms in the dressed state model is negligible [13,14].

Our measurements and calculations provide direct and quantitative spectroscopic information on both the intensity of spontaneous emission inside the atomic cloud, and on the atomic absorption/amplification cross section for these photons under very simple conditions (two level

[a] e-mail: fekhayko@wis.weizmann.ac.il

atom, one and uniform pump beam, controlled polarization). This information can be added to the indirect information inferred from measurements of atomic densities [6] and temperatures [15] and of fluorescence decay times [8] to improve our understanding of photon re-scattering, radiation trapping, light induced heating and repulsive forces in cold atomic clouds.

In the next section, the experiment for measuring the weak probe amplification and its saturation is described. In Section 3, our model for the saturation of the amplification is presented. Using this model, it is possible to calculate the saturation and its dependence on the intensity and the detuning of the pump laser. In Section 4 we summarize and suggest possible uses and improvements of our work.

2 Measurement of the saturation of amplification in a dense atomic cloud

To measure the modified absorption spectrum of excited atoms inside a cold and dense atomic cloud, we performed a pump-probe experiment on Rb atoms released from a magneto-optical trap (MOT). We measured the amplification of a weak probe beam, in the presence of a strong pump beam, as a function of the OD of the cloud and the parameters of the pump laser. The experimental setup is shown in Figure 1, and will be described here in some detail.

In the first stage, ^{85}Rb atoms were collected in a MOT from a Rb vapor with partial pressure of $\sim 3 \times 10^{-9}$ torr. Variable loading time served to control the OD of the atomic cloud between 1 and 30. The maximal number of atoms was 5×10^8, and the maximal MOT $1/e$ diameter was 2.8 mm. After the variable loading time, the six MOT beams and the magnetic field gradient were shut off, within less than 500 μs. The temperature of the atoms was measured to be 150 μK. This corresponds to a Doppler broadening of 155 kHz (FWHM) which is much smaller than the natural linewidth of 6 MHz.

Next, a single pump laser beam was turned on, with an intensity $I = 64\, I_{\rm sat}$ ($I_{\rm sat} = 1.65$ mW/cm^2 is the saturation intensity) and a pulse length of 50 μs. The size of the pump beam (1.2 cm $1/e$ diameter) was much larger than the atomic cloud to ensure uniform pump intensity[1]. Simultaneously, a short pulse of the weak probe laser ($I = 0.08\, I_{\rm sat}$) was applied to the atomic cloud. The probe pulse was short (7 μs) so that the Doppler shift of the atoms, which are accelerated by the pump beam, could be neglected. The probe frequency was scanned during the pulse, with a slope of 30 MHz/μs, to cover the three $5S_{1/2}$, $F = 3 \rightarrow 5P_{3/2}$, F' lines (with $F' = 2$, 3, and 4). Its transmission spectrum was measured by a photomultiplier tube, and recorded on a digital oscilloscope. The diameter of the probe beam was 1.4 mm, and it was aligned carefully through the center of the cloud, to obtain the maximal amplification and optical density.

[1] Due to its large intensity, the pump attenuation is small even for the large OD.

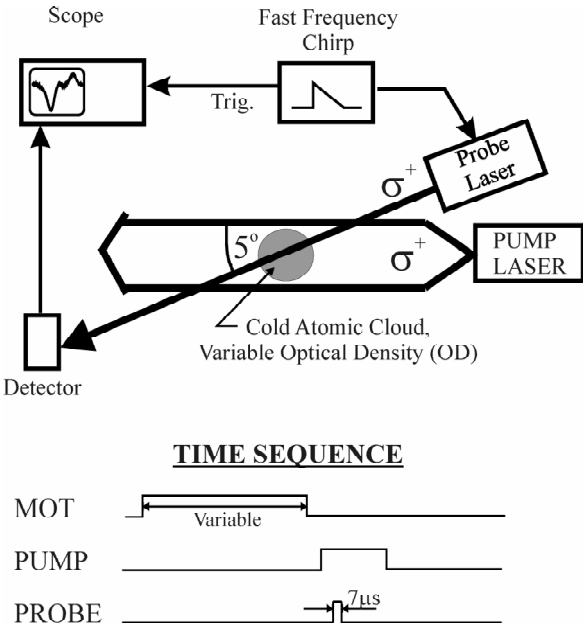

Fig. 1. The experimental setup. The cold atomic cloud is released from a MOT after a variable loading time, to control its OD. Pulsed pump and probe lasers are implied simultaneously. The probe pulse width is 7 μs, its frequency is scanned very fast during the pulse, and its transmission through the cloud is measured as a function of frequency. Both lasers have the same circular polarization, and the angle between them is small ($\sim 5^\circ$).

To obtain the clearest experimental situation, we assured that the atoms could be treated as two-level atoms. Hence, we took care to produce the same circular polarization (say σ^+) for both the probe and pump lasers, and to keep the angle between the two beams very small ($< 5^0$)[2]. The most reliable evidence that a two-level situation was indeed obtained was given by the absorption spectrum itself. A narrow (< 1 MHz) dispersive signal in the absorption spectrum, at the pump laser frequency, was observed when the probe polarization was not σ^+, indicating Raman transitions between different magnetic sub-levels of the ground state, as in references [4,5,16]. When the probe polarization was exactly σ^+ (as measured optically) the dispersive Raman signal completely disappeared and the measured absorption spectrum showed good quantitative agreement with the two-level theory [2] for clouds with small OD.

We measured the modified absorption spectrum of the $F = 3 \rightarrow F' = 4$ transition in the presence of the strong pump. The pump frequency was detuned above the atomic transition frequency, so that the Mollow

[2] In the presence of the strong and circularly polarized pump beam, and with nearly zero magnetic field (< 50 mG), a well defined quantization axis exists. Moreover, optical pumping quickly populates only the $F = 3$, $m_F = 3$ magnetic sublevel which is only connected to the $F' = 4$, $m_{F'} = 4$ sublevel. Finally, a weak repumping beam on resonance with the $F = 2 \rightarrow F' = 2$ line depletes all the $F = 2$ states.

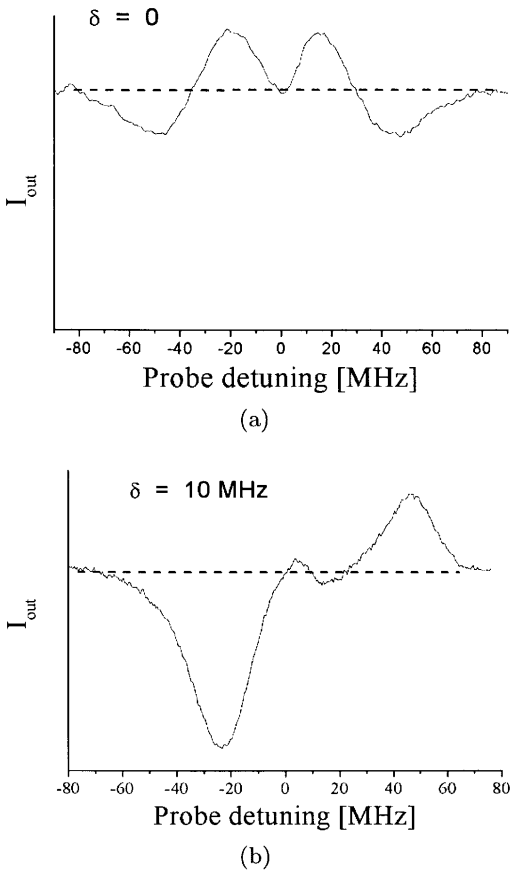

Fig. 2. Examples of two measured transmission spectra, (a) for a detuning $\delta = 0$ of the pump laser, (b) for $\delta = 10$ MHz.

amplification would not interfere with the modified $F = 3 \rightarrow F' = 3$ line. Two examples of the measured spectra for $OD = 30$ are shown in Figure 2, for two different detunings of the pump laser: $\delta = 0$ and $\delta = 10$ MHz. These spectra show the same qualitative features of absorption and amplification as in the low OD case, but the height and width of these features change, as discussed below. The wide dispersion line in Figure 2b, which is caused by two-photon spontaneous emission processes, is well understood from the two-level Mollow theory [2,14]. From the measured spectrum, we calculated the Rabi frequency of the pump beam, and found it to be 34 MHz, in agreement with the measured intensity of the pump laser. The spectrum was then recorded for different OD of the atomic cloud, and for different pump detunings in the range $0 < \delta < 45$ MHz, and the peak amplification was measured. To measure the OD, we closed the pump laser and performed a weak probe absorption measurement. OD is defined as $OD = -\ln(I_{\rm out}/I_{\rm in})$ for the $F = 3$, $m = 3 \rightarrow F' = 4$, $m' = 4$ transition. For high OD the absorption of the strong line ($F = 3 \rightarrow F' = 4$) was much larger than 99% and difficult to measure directly. Therefore, we measured the maximum absorption at the weakest line ($F = 3 \rightarrow F' = 2$) and normalized it by

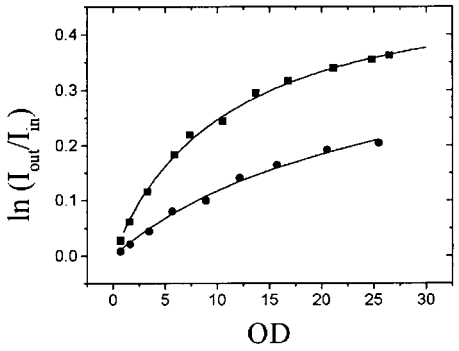

Fig. 3. Measured amplification as a function of the OD of the cloud for two pump detunings: $\delta = 10$ MHz (■) and 33.4 MHz (●). The fits according to equation (1), plotted in solid curves, yield: $A = 0.047$, $B = 0.093$ for $\delta = 10$ MHz and $A = 0.016$, $B = 0.013$ for $\delta = 33.4$ MHz.

the ratio between the proper Clebsh-Gordon coefficients[3]. The maximal OD of 30, is in good agreement to the value calculated from the measured number of atoms and cloud size.

Two examples of the measured peak amplification $\ln(I_{\rm out}/I_{\rm in})$ as a function of OD are shown in Figure 3, for detunings of $\delta = 10$ MHz and 33.4 MHz of the pump laser from resonance. As seen, amplification as high as $\sim 40\%$ was measured for the highest OD. A clear deviation from linear dependence is observed in the experimental data indicating the existence of strong saturation. The data was fitted with the expression:

$$\ln\left(\frac{I_{\rm out}}{I_{\rm in}}\right) = \frac{A \cdot OD}{1 + B \cdot OD}\,. \qquad (1)$$

These fits, also plotted in the graph, describe the data very accurately. The coefficient A in equation (1) is the amplification coefficient in small OD, and can be calculated directly from the Mollow theory. The coefficient B is the saturation coefficient, which is derived in the next section.

The fitting was repeated for all values of δ. The measured amplification was well fitted by equation (1) in all cases and the coefficients A and B were found. The measured amplification coefficient A as a function of δ is shown in Figure 4. Probe amplification for small OD is not a new result. It was already measured for an atomic beam [3] and in dilute atomic clouds [4]. We present it here, because the excellent agreement with theory confirms the accuracy of both our OD and peak amplification measurements. In Figure 5, the measured saturation coefficient B is shown as a function of the detuning of the pump laser. Values as high as 0.09 were measured for B, which means that for a cloud with $OD = 30$, the amplification drops to 27% of its unsaturated value.

[3] $C_{3344}/\frac{1}{m}\sum_m C_{3m2m+1} = 19$, where $C_{FmF'm'}$ is the Clebsh-Gordon coefficient of the transition $F, m \rightarrow F', m'$. The average over the m states in the denominator represents random atomic polarization as indeed occurs with no pump. The normalization procedure was verified experimentally by comparing the absorption lines at small OD.

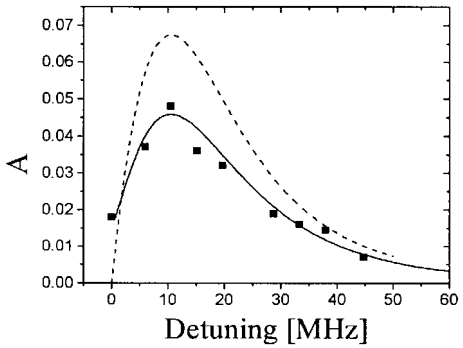

Fig. 4. Measured amplification coefficient, as a function of the pump detuning (■). The pump intensity was equal for all the detunings ($\Omega_{\rm Rabi} = 34$ MHz). The dashed curve is given by the dressed atom model (Eq. (8)), and the solid curve is calculated numerically from the Mollow theory following reference [2].

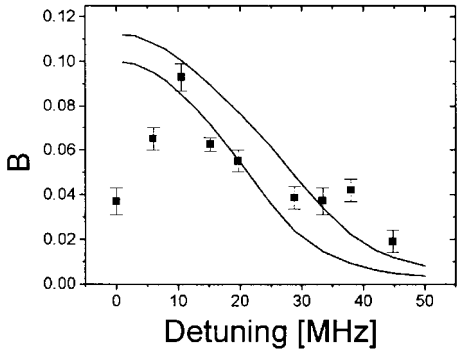

Fig. 5. Measured saturation coefficient, as a function of the pump detuning (■). The error bars are obtained from the statistical error of the fit to the data. The pump intensity was equal for all the detunings ($\Omega_{\rm Rabi} = 34$ MHz). The solid lines show the calculated saturation coefficient, as described in the text with a geometrical factor $\langle g \rangle = 0.9$ (upper curve) and $\langle g \rangle = 0.8$ (lower curve).

3 Theory

Our model for the saturation of weak probe amplification treats the combined atom-laser system using the dressed atom approach [13]. The model is based on changing the rate equations for the reduced populations of the dressed states, to include the influence of the re-absorption and amplification of spontaneously emitted photons. Throughout this section, the case of $\delta > 0$ will be treated ($\delta < 0$ yields identical results). In Figure 6 two manifolds from the infinite ladder of the dressed states are shown. Π_1 and Π_2 are the reduced populations of the dressed states, the two sidebands of the spontaneous emission spectrum are at frequencies $\omega_{\rm L} + \Omega_{\rm eff}$ and $\omega_{\rm L} - \Omega_{\rm eff}$, and the decay rates are Γ_{12} and Γ_{21} ($\Omega_{\rm eff} = \sqrt{\Omega_{\rm Rabi}^2 + \delta^2}$ where $\Omega_{\rm Rabi}$ is the Rabi frequency of the pump laser). For $\delta > 0$, the populations satisfy $\Pi_1 > \Pi_2$ as seen in the figure [13]. As a result, a weak probe beam tuned to resonance with the $1 \rightarrow 2$ dressed-level transition is absorbed, and a weak probe tuned to resonance with the $2 \rightarrow 1$ transition is amplified.

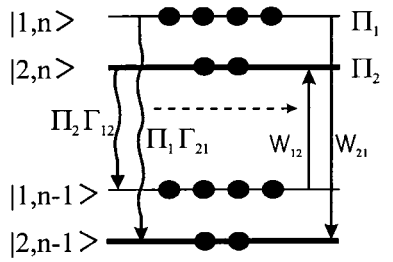

Fig. 6. Two manifolds of the dressed energy levels. Shown are the population $\Pi_1 > \Pi_2$, the transition rates between them due to spontaneous emission ($\Pi_2\Gamma_{21}$ and $\Pi_1\Gamma_{12}$) and its re-absorption (W_{12}) and amplification (W_{21}).

When the optical thickness of the atomic cloud increases in all directions, the probability to re-scatter spontaneously emitted photons becomes very large. Since the two Mollow fluorescence sidebands are in resonance with the dressed level transitions, re-scattering these photons affects the populations of the dressed states. The central Mollow band, as well as the elastic Rayleigh scattering peak, do not affect the dressed state population and are therefore not treated here (in other experimental situations they may be very important [8]). To describe the effect of re-scattering, we included in the model the rates for absorption and amplification of spontaneously emitted photons, W_{12} and W_{21}, respectively. Adding these two processes into the population rate equations changes the steady state solutions, and causes a saturation of the peak probe amplification.

In the following, we will consider spontaneously emitted photons that are re-scattered by an atom as a small perturbation, which only influences the population difference between the dressed states, without perturbing the dressed-atom energy levels and the decay rates[4]. We mainly analyze a one-dimensional (1D) situation, in which the spontaneously emitted photons can propagate only parallel to the x-axis (in the forward or backward directions). We also assume uniform atomic density, uniform pump intensity and uniform dressed level populations across the cloud. The last assumption is over-simplified, since spatial modes of the level population are expected for large OD. However, since these spatial modes are often slowly varying [8], we may consider the average level population as a good approximation. With these assumptions the modified dressed-states population rate equations are (see Fig. 6)

$$\begin{cases} \dot{\Pi}_1 = -\Gamma_{21}\Pi_1 + \Gamma_{12}\Pi_2 - W_{21} - W_{12} \\ \dot{\Pi}_2 = \Gamma_{21}\Pi_1 - \Gamma_{12}\Pi_2 + W_{21} + W_{12} \end{cases} . \qquad (2)$$

Note that the strong pump laser introduces no transitions between the dressed state levels since they are eigen states of the total atom + pump laser Hamiltonian.

[4] The perturbation can be described as small, when the condition of weak absorption of the pump laser is fulfilled.

The absorption rate W_{12} is now evaluated using the dressed atom model (a similar expression is then obtained also for the amplification rate W_{21}). The flux of photons that are re-scattered in the absorption sideband, per unit area, from a thin slice dx of the cloud is $(1/2)\Gamma_{12}\Pi_2 n\mathrm{d}x$, where n is the atomic density [13]. The factor $1/2$ is needed because in the 1D case, only half of the re-scattered photons move in the direction of the atom. Multiplying this flux by the absorption cross-section $\sigma_{\rm abs}$ gives the absorption rate by a given atom, for scattered photons from the thin slice. The total re-absorption rate, W_{12}, for an atom in the cloud center ($x = 0$) is calculated by integrating the contribution from the thin slices along the atomic cloud to yield,

$$W_{12} = \frac{1}{2}\Gamma_{12}\Pi_2 n\sigma_{\rm abs} 2\int_0^{L/2} \mathrm{d}x\, \exp(-\sigma_{\rm abs} n x), \qquad (3)$$

where L is the cloud length. The decay of the photon flux due to the absorption of the spontaneous photons along the cloud, $\exp(-\sigma_{\rm abs} n x)$, is large especially for large δ, since then $\sigma_{\rm abs} \to \sigma_0$. Note that frequency re-distribution during re-scattering is neglected here, as in reference [8] due to suppression of Doppler broadening.

To compare the model to the experimental results, it is convenient to use the OD of the atomic cloud as a variable. The OD of a cloud is equal to $\sigma_0 nL$, where σ_0 is the absorption cross-section of the bare atom. After multiplying and dividing by σ_0, and performing the integral over x, we get:

$$W_{12} = \Gamma_{12}\Pi_2 \left[1 - \exp\left(-\frac{1}{2} OD \frac{\Gamma_{12}\Delta\Pi}{\gamma}\right)\right]. \qquad (4)$$

Here, the normalized absorption cross-section of the dressed-atom model, $\sigma_{\rm abs}/\sigma_0 = \Delta\Pi\Gamma_{12}/\gamma$, was used [17], where γ is the natural line width of the atomic transition and $\Delta\Pi = \Pi_1 - \Pi_2$ is the dress state population difference. For the amplification sideband, the re-scattered photons are amplified in the cloud, with a normalized amplification cross-section of $\sigma_{\rm amp}/\sigma_0 = \Delta\Pi\Gamma_{21}/\gamma$, and the resulting re-amplification rate is:

$$W_{21} = \Gamma_{21}\Pi_1 \left[\exp\left(\frac{1}{2} OD \frac{\Gamma_{21}\Delta\Pi}{\gamma}\right) - 1\right]. \qquad (5)$$

It is possible now to find the steady state population difference, $\Delta\Pi$ in the presence of the spontaneous emission. Applying $\dot{\Pi}_{1,2} = 0$ in the rate equation (2) and using equations (4, 5) for W_{12} and W_{21}, yields a self consistent equation:

$$\begin{aligned} 0 = {} & \Delta\Pi(\Gamma_{12} + \Gamma_{21}) - (\Gamma_{12} - \Gamma_{21}) \\ & + \langle g\rangle(1 - \Delta\Pi)\Gamma_{12}\left[1 - \exp\left(-\frac{1}{2} OD \frac{\Gamma_{12}}{\gamma}\Delta\Pi\right)\right] \\ & + \langle g\rangle(1 + \Delta\Pi)\Gamma_{21}\left[\exp\left(\frac{1}{2} OD \frac{\Gamma_{21}}{\gamma}\Delta\Pi\right) - 1\right]. \end{aligned} \qquad (6)$$

A geometrical factor $\langle g\rangle$ was added to W_{12} and W_{21} to extend equation (6) to a more general geometry. Actually, even for our simple 1D case a geometrical factor is needed, since the re-absorption rate depends on the position of the absorbing atom. For an atom in the middle of the cloud, $\langle g\rangle = 1$, and a factor of $1/2$ is needed in the exponent, as in equations (4, 5). However, for an atom at the edge of the cloud, $\langle g\rangle = 1/2$, and the factor in the exponent is 1[5]. Since our model is spatially uniform, some average $\langle g\rangle$ should be used. For 3D geometry the flux of the spontaneous emission tends to decrease compared to the 1D values. For example, for low OD spherical atomic cloud this flux is reduced by a factor of 2 in the middle of the cloud, and by a factor of 3 toward its bounds. Nonetheless, when the OD of the cloud for spontaneous photons becomes much larger than one, the re-absorption rate becomes less dependent on the position of the absorbing atom, and the value of $\langle g\rangle$ is expected to grow and reach its 1D value of one (in our experiment the probe beam is smaller than the cloud and passes through its center, which further supports the use of the 1D model).

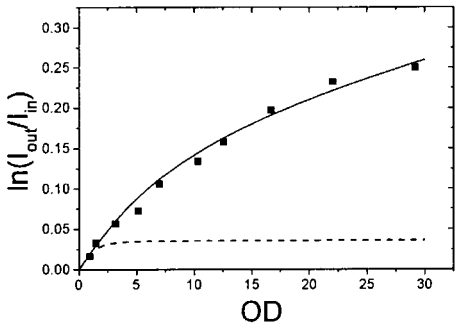

Fig. 7. Amplification of the probe beam as a function of OD as calculated from self-consistent model based on dressed atom (solid line), compared to the measured values (■) for $\delta = 28.8$ MHz and $\Omega_{\rm Rabi} = 34$ MHz. The dashed line shows the modified model that does not include multiple scattering of spontaneous emission, and clearly does not reproduce the data.

To compare the model with the experimental data, the amplification of a weak probe laser with a frequency $\omega_{\rm L} + \Omega_{\rm eff}$ by the cloud was calculated as:

$$\frac{I_{\rm out}}{I_{\rm in}} = \exp\left(\frac{\sigma_{\rm A}}{\sigma_0} OD\right) = \exp\left(\frac{\Delta\Pi\Gamma_{21}}{\gamma} OD\right), \qquad (7)$$

where $\Delta\Pi$ was calculated numerically from equation (6), for the pump parameters of the experiment. The results of that calculation, for $\delta = 28.8$ MHz are shown in Figure 7, together with the experimental data. The model was normalized to the correct amplification value as given from the exact calculation of Mollow [2], and is shown for $\langle g\rangle = 0.87$, which gave best fit to the data. This procedure was repeated for all the pump detunings used in the experiment and similar agreement to the measured amplification was found. The values of the adjustable parameter $\langle g\rangle$ changed by $\pm 8\%$ while fitting the data for all $\delta > 10$ MHz, with an average value of $\langle g\rangle \sim 0.85$.

[5] This can be seen by changing the limits of the integral in equation (3) to $[0\, L]$.

For lower detunings, the model could still fit the data, but with smaller values of $\langle g \rangle$.

The inclusion of the multiple scattering of the scattered photons in the model is crucial for the high OD. To emphasize the importance of this process, we tried to fit the data with a modified model in which we assume that incident photons are unlikely to scatter more than twice and therefore use $\exp(-\sigma_{\rm abs} nx) \sim \exp(\sigma_{\rm amp} nx) \sim 1$ in the derivation of W_{12} and W_{21}. The amplification *vs.* OD calculated from this model for $\delta = 28.8$ MHz, with $\langle g \rangle = 0.87$, is also shown in Figure 7. At $OD < 2$, the two models give the same values, indicating that multiple scattering in that range is small. However, for higher OD the modified model predicts huge saturation that is not supported by the data.

To compare our model to the experimental data for various δ, it is useful to parameterize the amplification and its saturation by the two coefficients of equation (1). These parameters indicate the amplification for small OD of the cloud (A), and the amount of saturation at large OD (B). The coefficient A can be evaluated analytically by expanding equation (6) for low OD to be

$$A = \frac{\Delta\Pi_0 \Gamma_{21}}{\gamma}, \tag{8}$$

where $\Delta\Pi_0 = (\Gamma_{12} - \Gamma_{21})/(\Gamma_{12} + \Gamma_{21})$ is the population difference for small OD (when photon re-scattering is negligible). Equation (8) is identical to single-atom treatments of weak probe amplification using the dressed state model [17], as expected. The dressed-state value for the amplification is shown in Figure 4, compared to the measured values. As seen, the model gives a good agreement to the data for large δ, but is unable to explain the behavior of the amplification for small δ[6]. The amplification coefficient can be evaluated more accurately using the exact absorption spectrum of a driven atom following Mollow [2]. This exact calculation is also shown in Figure 4 without any adjustable parameter. As expected, the measured amplification values for small OD are in excellent agreement with the Mollow theory for all δ, verifying the accuracy of our measurements.

Next we deal with the saturation coefficient B which represents the new physical mechanisms that emerge at high OD. The coefficient B was calculated by fitting the model with equation (1), using A from equation (8). The parameterization of B was repeated for all δ with a constant value for $\langle g \rangle$. The results are shown in Figure 5, for two values of $\langle g \rangle$ (0.8 and 0.9) and compared to the measured values. As seen, the model gives the correct value range for the saturation coefficient and its correct δ dependence for $\delta > 10$ MHz, with the single adjustable parameter $\langle g \rangle$ close to its 1D value of one.

Note that, although the exact model and its parameterized form describe the experimental data equally well (in Fig. 7 they would not be distinguishable) we do not claim any physical significance to the exact functional form of equation (1). We could fit the experimental data equally well also with other functional forms, in particular for the larger δ, where the lower amount of saturation reduced the constraints imposed by the scatter of the data.

For small δ our model fails, and does not predict the decrease of the saturation toward $\delta = 0$. This may be due to two factors. First, since the main mechanism for amplification for $\delta \leq \gamma$ is not related to dressed state population differences [14] (see discussion of Fig. 4) our model is not expected to treat it correctly. Second, for small δ, the cross-sections for re-scattering spontaneous photons are very small, and the cloud is nearly transparent even for the large OD. Therefore, the geometrical factor for a sphere (which is 2–3 times smaller than for our 1D model) should be used and a smaller saturation is thus expected. When δ is large, the large OD for spontaneous emission tends to increase $\langle g \rangle$ to its 1D value.

4 Conclusions

In this work we discovered a new saturation phenomena of weak probe amplification in a highly driven cold atomic cloud at high optical densities, that is caused by re-scattering of spontaneously emitted photons. We were able to describe our experimental data with a model that treats the atomic dressed state population and the intensity of spontaneous emission in the atomic cloud in a self-consistent manner. Self-consistency is required to describe nonlinear trapping under strong external excitation [12]. The model agrees with the data over a large range of laser pump detunings using a single adjustable parameter in the form of a geometrical factor (which was found to be close to the expected value). The model does not describe the data well for pump frequencies close to the atomic resonance, where nonsecular mechanisms that are not considered play a major role.

The amount of saturation predicted by our model is very sensitive to the intensity of spontaneous emission in the atomic could and to the atomic cross sections for absorption and amplification of this spontaneous emission. By performing the experiments with very simple conditions (single and uniform pump beam, effective two-level atoms, steady state conditions, well controlled polarization, negligible collision and Doppler broadening) we could accurately account for the light atom interaction and use the comparison between theory and experiment to investigate multiple scattering. Alternatively, similar experiments may be conducted on more complicated systems that can involve multiple and non-uniform pump beams, multi-level atoms, non-uniform magnetic fields, complicated polarization and dynamics. Weak probe amplification and its saturation can then serve as a new experimental tool for studying the radiation field and its interaction with the atoms in such complicated system.

An example for such a system is the MOT itself where multiple scattering induces strong repulsive forces between the atoms. These forces strongly depend on the very same re-scattering rates that cause the saturation in probe amplification. Existing models to describe these effects are mostly over-simplified and do not give an accurate

[6] For $\delta \leq \gamma$ the nonsecular terms in the dressed atom model, scaled as $\gamma/\Omega_{\rm R}$, give rise to amplification processes.

description of the MOT density [6,18]. We have observed saturation of weak probe amplification for a MOT under wide range of operating conditions, and found them in general to be smaller than here. Without such saturation (that signifies a reduction in atomic cross section to absorb re-scattered photons), the light-induced repulsive force would rapidly increase for very large MOTs where strong radiation trapping is observed [8].

Saturation of the reduced populations of the dressed states can affect not only the absorption spectra but also the fluorescence spectra at high optical densities. For example, our model predicts that the reduction of the population difference changes the balance between the two Mollow fluorescence sidebands at high OD inside the cloud. The re-absorption of spontaneous emission increases Π_2 and decreases Π_1, (for positive pump detunings) leading to enhancement of the $2 \rightarrow 1$ (absorbed) sideband. This effect is significant in large pump detunings, where initially $\Pi_1 \gg \Pi_2$. Future measurements of the spectrum of the spontaneous emission from a cold and optically dense atomic cloud together with absorption spectroscopy, may both serve as useful experimental techniques, complementary to temporal measurement technique of radiation escape times [8].

Finally, our model can be improved in several respects to present the physical situation more realistically (with the cost of higher complexity). These include non-uniform excitation profile that is expected to occur in systems with multiple scattering, full 3D geometry, frequency redistribution during re-scattering and non uniform atomic density. These factors can be taken into account by making the rates W_{12} and W_{21} to be dependent on the emission and absorption location. This will change equation (6) into an integral equation for $\Delta\Pi(r)$, which can be solved for the real geometry of the atomic cloud.

This work was supported in part by the Israel Ministry of Science, the Israel Science Foundation, and the Minerva Foundation. ND is an incumbent of the Rowland and Sylvia Scheafer career development chair.

References

1. B.R. Mollow, Phys. Rev. **188**, 1969 (1969).
2. B.R. Mollow, Phys. Rev. A **5**, 2217 (1972).
3. F.Y. Wu, S. Ezekiel, M. Ducloy, B.R. Mollow, Phys. Rev. Lett. **38**, 1077 (1977).
4. J.W.R. Tabosa, G. Chen, Z. Hu, R.B. Lee, H.J. Kimble, Phys. Rev. Lett. **66**, 3245 (1991).
5. M. Mitsunaga, T. Mukai, K. Watanabe, T. Mukai, J. Opt. Soc. Am. B **13**, 2696 (1996).
6. T. Walker, D. Sesko, C. Wieman, Phys. Rev. Lett. **64**, 408 (1990).
7. K. Ellinger, J. Cooper, P. Zoller, Phys. Rev. A **49**, 3909 (1994).
8. A. Fioretti, A.F. Molisch, J.H. Müller, P. Verkerk, M. Allegrini, Opt. Commun. **149**, 415 (1998).
9. Y. Castin, J.I. Cirac, M. Lewenstein, Phys. Rev. Lett. **80**, 5305 (1998).
10. T. Holstein, Phys. Rev. **72**, 1212 (1947); **83**, 1159 (1951).
11. M.G. Payne, J.E. Talmage, G.S. Hurst, E.B. Wagner, Phys. Rev. A **9**, 1050 (1974).
12. N.N. Bezuglov, A.N. Klucharev, A.F. Molisch, M. Allegrini, F. Fuso, T. Stacewicz, Phys. Rev. E **55**, 3333 (1997).
13. C. Cohen-Tannoudji, J. Dupon-Roc, G. Grinberg, *Atom-Photon Interactions* (Wiley, New York, 1992), Chap. 6.
14. G. Grinberg, C. Cohen-Tannoudji, Opt. Commun. **96**, 150 (1993).
15. C.J. Cooper, G. Hillebrand, J. Rink, C.G. Townsend, K. Zetie, C.J. Foot, Europhys. Lett. **28**, 397 (1994).
16. D. Grison, B. Lounis, C. Salomon, J.Y. Courtois, G. Grynberg, Europhys. Lett. **15**, 149 (1991).
17. C. Cohen-Tannoudji, S. Reynaoud, J. Phys. B **10**, 345 (1977).
18. C.G. Townsend, N.H. Edwards, C.G. Cooper, K.P. Zetie, C.J. Foot, A.M. Steane, P. Szriftgiser, H. Perrin, J. Dalibard, Phys. Rev. A **52**, 1423 (1995).